Chemical amplification of sub-threshold base triggers to drive sol-gel transitions in polymers

Shuqi Lai, Gaurav Chaudhary, Zhelong Jiang, Randy H. Ewoldt, Paul V. Braun*

ABSTRACT: Chemical amplification has been widely applied in applications ranging from stimuli sensing to advanced photoresists but is rarely utilized to drive productive mechanical property changes. Here we demonstrate the use of a base amplifier to drive gelation of a functional polymer solution in response to a sub-threshold base trigger through a mechanism whereby the trigger drives a dramatic increase in the base concentration driven by base amplification, resulting in complexation of Fe(III) and polymer-bound catechol groups and subsequent gelation of the polymer solution. The concomitant crystallization of dibenzofulvene, a byproduct of base amplification, led to significant stiffening of the resultant gel and an unexpected temperature-sensitive change of gel stiffness.

Stimuli amplification is ubiquitous in biology and common in engineered systems ranging from sensors to machines.[1–4] While biology often utilizes a complex chemical cascade to convert a weak signal into a strong response,[5] engineered systems typically rely on electronics to amplify weak signals. Interesting emerging examples of synthetic chemical systems that can amplify weak chemical stimuli include those chemistries which improve sensitivity to for example F^-[6,7] and thiol.[8] Common to these and other emerging systems which amplify chemical stimuli is to use autocatalytic reactions triggered by the initial signal inputs. In such an approach, the same chemical species as the initial trigger is released via autocatalytic decomposition of stimuli amplifier molecules, sustaining the reactions till full consumption of the stimuli amplifier.[9] In the sensing space, a majority of such efforts have been focused on detection and quantification of dilute analytes.[10–12] It is our postulate, and the focus of the work presented here, that the concept of application of autocatalytic amplification reactions to change the properties of materials is considerably underdeveloped, and that after appropriate development can be utilized to trigger chemical reactions that significantly modify mechanical properties of a material.

We specifically selected bases as the chemical stimuli of interest. In the presence of a base trigger, autocatalytic decomposition of a base amplifier (BA) generates one or more equivalents of base molecules relative to BA molecules per cycle, leading to an exponential increase in base concentration. Following the pioneering work of Arimitsu and Ichimura *et al.*,[13,14] diverse chemistries of BAs have been devised.[15–17] The versatility of bases in chemical reactions have led to the employment of BAs in applications including photolithography,[18,19] resin curing,[20,21] frontal free radical polymerization,[22,23] and degradable polyurethanes.[17,24] However, in the published systems, the amplification reactions occurred at elevated temperatures and/or a stoichiometric amount of a base trigger was applied.

Here we apply a base amplifier to amplify a dilute base trigger (4-benzylpiperidine, BPD) at a moderate temperature (≤40 °C). The BPD concentration was specifically selected to be at such a low level that it alone does not result in a measurable change in the mechanical properties of the host system. Only if the BPD stimulus is subsequently amplified will there be a productive mechanical response, i.e., sol-gel transition and stiffening of a functional polymer solution. To design a responsive host where the mechanical response is specifically the result of the amplified change of base concentration, we deliberately chose catechol-Fe(III) complexation as the reaction which converts the change in base concentration to a mechanical property change. This reaction occurs readily at a moderate temperature (≤40 °C) and does not require the presence of any co-catalyst. The nature of the catechol-Fe(III) complexation is a strong function of pH or base concentration. In an acidic medium, Fe(III) tends to bind catechol in a 1:1 ratio. As base concentration increases, the complexation ratio (Fe(III) : catechol) shifts to 1:2 and eventually 1:3. When catechol groups are tethered to a polymer backbone, formation of bis- and tris-catechol-Fe(III) complexes leads to non-covalent crosslinks which can induce gelation of the polymer solution.[25]

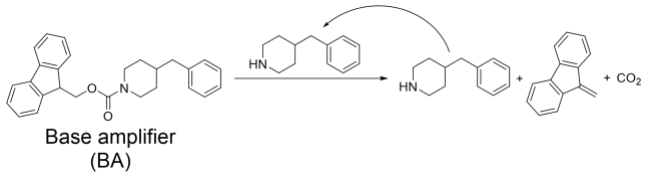

Figure 1. Base-triggered autocatalytic decomposition of BA.

Base Amplification in Functional Solutions. The base amplifier used here is derived from BPD, which, as demonstrated by He *et al.*,[23] decomposes autocatalytically in the presence of a base trigger, yielding an additional equivalent of BPD that continues to trigger decomposition of remaining BA molecules (Figure 1). Formed as

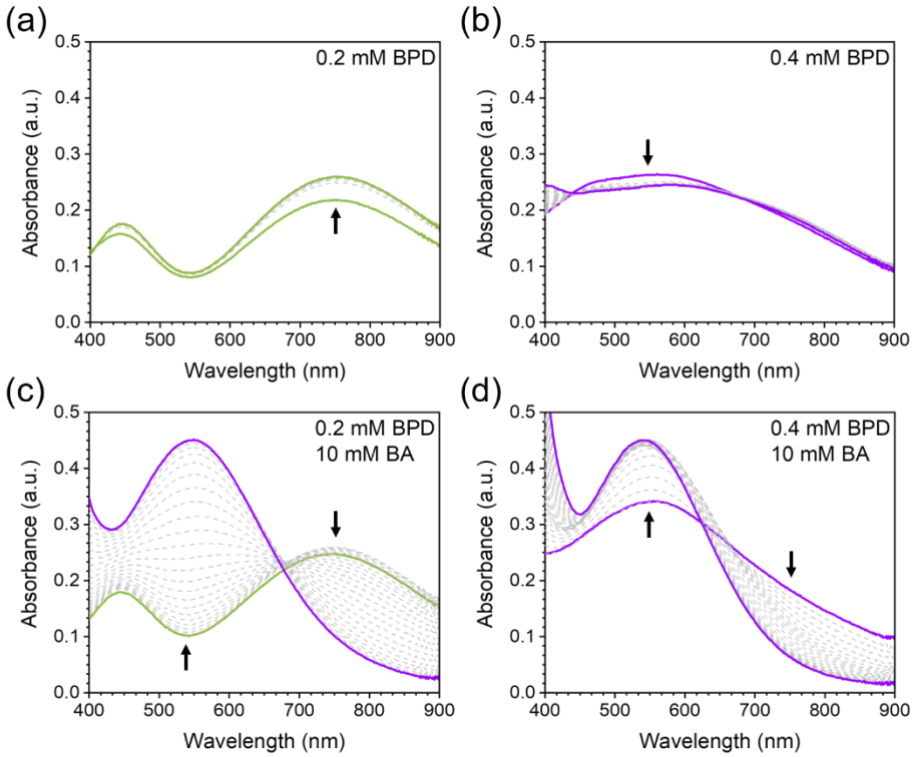

Figure 2. Time-lapse UV-Vis spectra of DMSO solutions of (a) 0.2 mM effective BPD, (b) 0.4 mM effective BPD, (c) 0.2 mM effective BPD + 10 mM BA, and (d) 0.4 mM effective BPD + 10 mM BA. All solutions contain 22 μg/mL $FeCl_3$, 44.8 μg/mL pyrocatechol (pyrocatechol/Fe = 3/1, mol/mol), and 1 mM TFA. Spectra were collected every 5 min for 2 hours at room temperature. The first and last spectra are highlighted by solid lines in colors of corresponding solutions, and arrows indicate directions of spectral evolution.

byproducts are dibenzofulvene (DBF) and CO_2. While a base is able to initiate both crosslinking and degradation of functional polymers,[26–28] we focused on utilizing a base in a constructive way to demonstrate the concept of base amplification in a base crosslinkable chemistry. Theoretically, base amplification is compatible with any base-involving reactions that are catalyzed by a base or that consume the base more slowly than base accumulation. Catechol-Fe(III) complexation was chosen as a functional manifestation because of its dependence on base concentration, and formation of the three possible catechol-Fe complexes can be monitored via UV-Vis spectroscopy.[25,29]

To confirm compatibility of the two chemistries, reaction monitoring of base-triggered BA decomposition was conducted in a DMSO solution of $FeCl_3$ and pyrocatechol (pyrocatechol/Fe = 3/1, mol/mol) containing 1 mM trifluoroacetic acid (TFA) using UV-Vis spectroscopy. When the amount of the base trigger was barely sufficient to neutralize TFA, BA-free and BA-containing solutions both showed minimal spectral changes with the mono-catechol-Fe(III) as the dominant species (Figure S1). The amount of BPD added in excess of 1.0 mM contributed to an effective base concentration that triggered decomposition of BA and further shifting of the equilibrium of pyrocatechol-Fe(III) complexation. In BA-free solutions, an equilibrium was reached within minutes (Figure 2(a)-(b)). At an effective BPD concentration of 0.2 mM, the green mono-pyrocatechol-Fe(III) complex formed in a BA-free solution resulting in an absorption peak at 751 nm. At an effective BPD concentration of 0.4 mM, an absorption peak at 560 nm associated with the bis-pyrocatechol-Fe(III) complex was observed.[25] The absorption at 398 nm was possibly attributed to formation of *o*-quinone from oxidation of catechol by Fe(III) in an alkaline environment.[30] Since *o*-quinone cannot coordinate with Fe(III), a concomitant decrease of the absorption peak at 560 nm was observed.

In contrast, when the effective base concentration was non-zero, the spectra of BA-containing samples kept evolving within the 2-hour experimental window (Figure 2(c)-(d)). Specifically, absorbance of the mono-pyrocatechol-Fe(III) complex at 751 nm decreased, while that of the bis-pyrocatechol-Fe(III) one at 550 nm increased even in the case of 0.2 mM effective BPD. The peak at 550 nm started to blueshift in the end of the 2-hour measurement, indicating formation of the tris-pyrocatechol-Fe(III) complex. The absorbance increase at low wavelengths could be due to accumulation of the DBF byproduct.[10] Notably, both BA-containing solutions reached similar final states despite different amounts of BPD that were added, because the maximum amount of BPD was mostly determined by the BA concentration, which was the same in both solutions and in large excess relative to the initial base trigger.

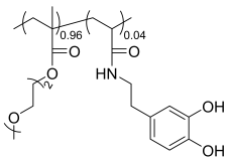

Figure 3. Chemical structure of poly[di(ethylene glycol) methyl ether methacrylate-co-dopamine acrylamide] (PDD).

Shown in Figure 4(a) is modulus evolution of a PDD solution containing $FeCl_3$ and 0.6 M BA upon addition of various sub-threshold concentrations of BPD. At t = 0, the base trigger was added to the polymer solution to initiate the amplification process. After an induction period with noisy data below the instrument torque limit, an abrupt modulus increase occurred due to sol-gel transition of the sample as base amplification proceeded and base

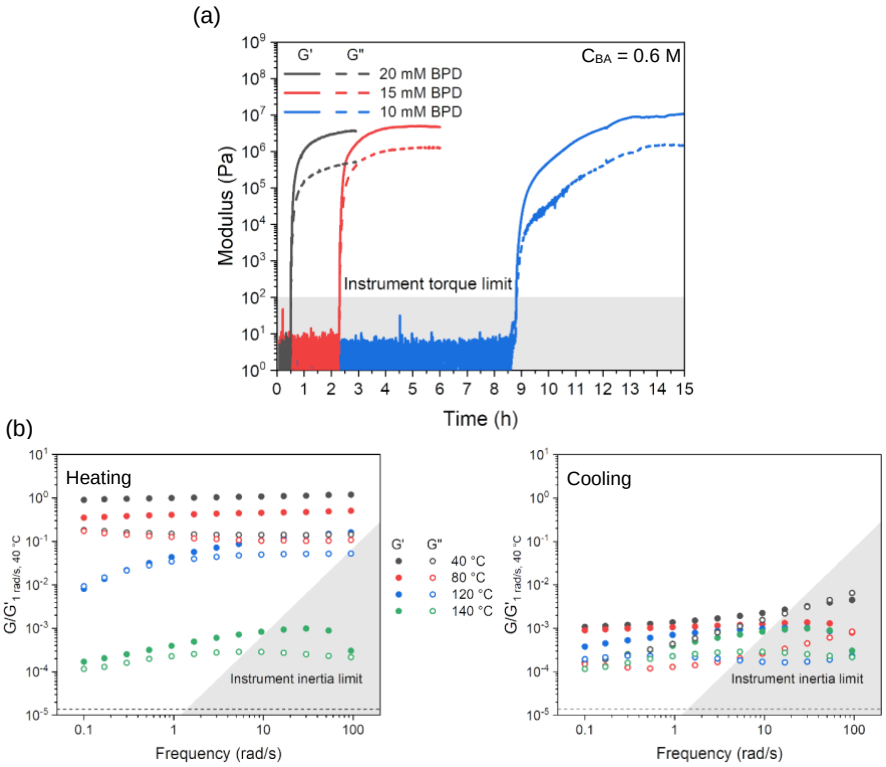

Figure 4. (a) Modulus development of 10 wt% PDD/DMSO solutions containing $FeCl_3$ (catechol/Fe = 3/1, mol/mol), 0.6 M BA, and 1 mM TFA upon triggering with different amounts of BPD at 40 °C. Data in the gray area is below the instrument torque limit. (b) Frequency sweeps of the organogel formed in response to 20 mM BPD during heating (40-140 °C, left) and cooling (140-40 °C, right). G' and G" were normalized to G' at 1 rad/s at 40 °C before the thermal cycle. Data in the gray area is below the instrument inertia limit, and the dashed line indicates the instrument torque limit.

Sol-Gel Transition of a Base-Amplified System. Now that compatibility of catechol-Fe(III) complexation and base amplification was confirmed, sol-gel transition of a functional polymer (poly[di(ethylene glycol) methyl ether methacrylate-co-dopamine acrylamide] (PDD), Figure 3) solution containing BA and $FeCl_3$ when triggered with a dilute base trigger was investigated using rheological characterization. The molar ratio of catechol group to Fe(III) was fixed at 3:1 for all tests, which allowed faster gelation kinetics over other ratios.[31] While both base amplification and catechol-Fe(III) complexation can proceed at room temperature, all measurements were done at 40 °C to shorten the timeframe of kinetics studies.

When there was only BA or 20 mM BPD in the polymer solution, no visible phase change was observed after 24 h at 40 °C (Figure S2), suggesting reasonable thermal stability of BA at the test temperature in the absence of a base trigger as well as the inability of 20 mM BPD alone to induce sol-gel transition. Over 20 mM BPD would induce immediate inhomogeneous gelation of the solution. Therefore, in this context, BPD concentrations no higher than 20 mM are called sub-threshold.

accumulated. Later, storage and loss moduli (G' and G" respectively) leveled off, indicating completion of the base amplification reaction. As a result of the fast transition process, the crossover point of G' and G" was buried in the noisy signals during the induction period. Thus, for practical purposes, we define the apparent gelation point as when G' first reached 100 Pa. When a more dilute BPD solution was used as the trigger, the induction period increased correspondingly, which is characteristic of an autocatalytic reaction.[32,33] As BPD concentration was decreased to 5 mM (BA/BPD = 120, mol/mol), gelation was not observed until several days later. Nonetheless, all three samples reached very similar plateaus, and the plateau G' was on the order of several MPa, which is 2 orders of magnitude higher than the maximum theoretical value from rubber elasticity theory (27.60 kPa, see SI for calculation). Such deviation implies contributions of factors other than catechol-Fe(III) complexation to mechanical properties of the organogel. Note, it was not possible to collect rheological data on gelation triggered by 5 mM BPD since gelation takes days in that case, and the solvent partially evaporates. Solvent evaporation is also

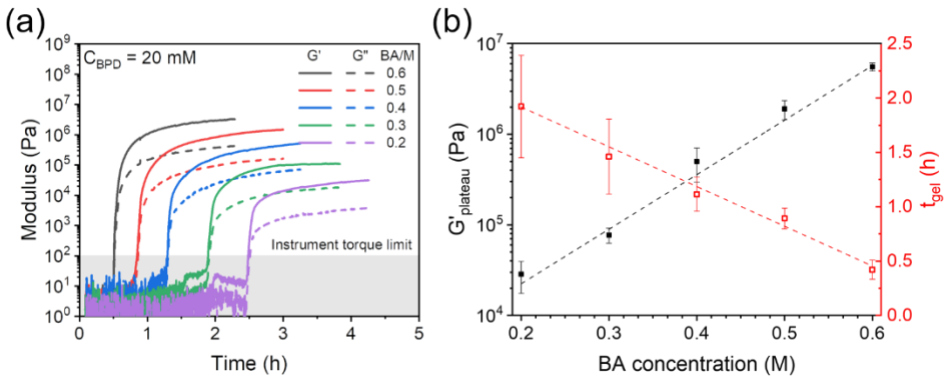

Figure 5. (a) Modulus development of 10 wt% PDD/DMSO solutions containing $FeCl_3$ (catechol/Fe = 3/1, mol/mol), different concentrations of BA, and 1 mM TFA upon triggering with 20 mM BPD at 40 °C. Data in the gray area is below the instrument torque limit. (b) Plateau storage moduli ($G'_{plateau}$) and gel times (t_{gel}) of samples in (a) against BA concentrations. Dashed lines are linear fit of data points (R^2 = 0.99 for log$G'_{plateau}$, and R^2 = 0.97 for t_{gel}). n=3.

why we suspect there appears to be multiple plateau moduli in the system triggered by 10 mM BPD.

Frequency sweeps were performed on the resultant gel at various temperatures (Figure 4(b)). At low temperatures, G' and G" showed little frequency dependence, indicating much slower exchanging kinetics of catechol-Fe(III) complexes in the resultant organogel than in a hydrogel[25] or in a BA-free organogel prepared by direct base addition (Figure S3(a)). As the temperature increased, exchange of catechol-Fe(III) complexes was kinetically unlocked and we observed a viscoelastic liquid terminal regime of G' and G" at low frequencies at 120 °C. When the sample was cooled down back to 40 °C, the sample returned to its gel state as indicated by G' > G" over a broad frequency range down to 0.1 rad/s. However, neither of the storage and loss moduli recovered to the original level. In contrast, when a BA-free organogel prepared by direct base addition was subjected to the same thermal cycle, an increase in storage modulus was observed at high temperatures, and after the thermal cycle, the final storage modulus at 40 °C was higher than the initial value, likely owing to oxidation of catechol groups by Fe(III) and resultant formation of chemical crosslinks (Figure S3(b)).

When the same amount of base trigger was used and BA concentration decreased, the gelation time (t_{gel}) increased linearly; meanwhile, the plateau storage modulus ($G'_{plateau}$) decreased exponentially and approached the maximum theoretical value (27.60 kPa) when the BA concentration was 0.2 M (Figure 5). In some cases, a small modulus increase was observed before the main jump, which led to a low plateau with G' higher than G". A similar phenomenon was observed in the bubble nucleation stage of polyurethane foaming and can be explained by formation of bubble network.[34,35] The gel times and plateau storage moduli of BA-containing samples triggered by various concentrations of BPD were summarized in Table S1.

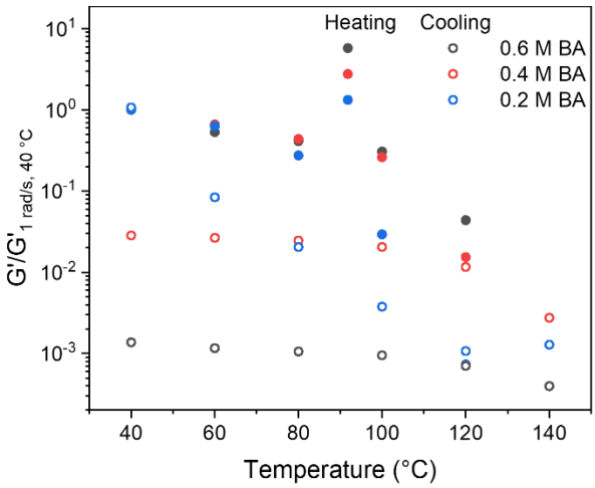

Figure 6. Normalized storage moduli of organogels formed after base amplification (20 mM BPD, 0.2-0.6 M BA) during a 40-140-40 °C thermal cycle. G' was measured at 1 rad/s and 0.1% strain and normalized to G' of each sample at 1 rad/s at 40 °C before the thermal cycle.

Figure 6 displayed evolution of storage moduli of selective gels during a 40-140-40 °C thermal cycle is displayed in. For each sample, the data was normalized to G' at 1 rad/s at 40 °C before the thermal cycle (Table S1). For all the samples, G' dropped drastically as temperature increased. With a lower BA concentration, the extent of G' recovery after the heating-cooling cycle was higher. Only when the BA concentration was as low as 0.2 M did the moduli before and after the heating-cooling cycle overlapped, despite some extent of hysteresis.

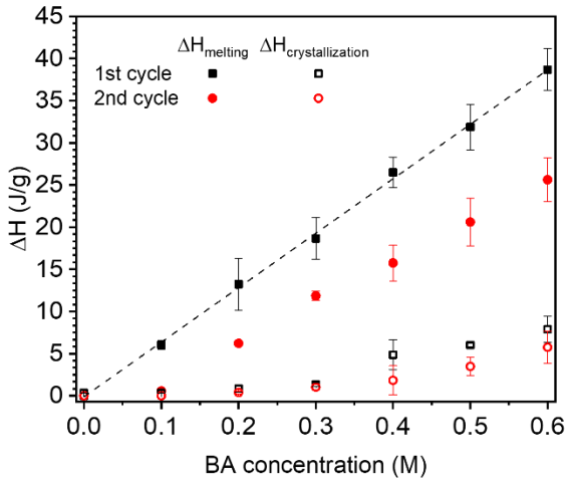

Figure 7. Enthalpies of melting ($\Delta H_{melting}$) and crystallization ($\Delta H_{crystallization}$) of organogels formed after base amplification (20 mM BPD, 0-0.6 M BA) against BA concentrations. Samples were subjected to 20-140-20-140-20 °C heating-cooling cycles at 5 °C/min. The dashed line is the linear fit of $\Delta H_{melting,1}$ ($R^2 = 1.00$). n=3.

Crystallinity of Organogels. Differential scanning calorimetry (DSC) was used to study thermal properties of the organogels formed after base amplification. An endothermic melting peak was observed at 112-116 °C, which shifted slightly to a higher temperature as the BA concentration decreased; when the samples were cooled down, an exothermic peak was observed at 40-50 °C (Figure S4). Shown in Figure 7, the enthalpy of melting ($\Delta H_{melting}$) was proportional to the initial BA concentration. After the first heating-cooling cycle, $\Delta H_{melting}$ decreased, accompanied by shifting of the endothermic melting peak to a lower temperature. The fact that the enthalpies of crystallization ($\Delta H_{crystallization}$) in both cycles were significantly smaller than $\Delta H_{melting}$, together with the decreasing $\Delta H_{melting}$, implies incomplete recovery of sample crystallinity.

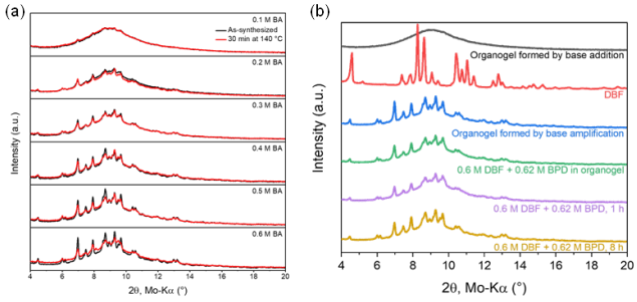

Figure 8. (a) XRD patterns of organogels formed after base amplification (20 mM BPD, 0.1-0.6 M BA) at 40 °C (black) and after another 30 min heating at 140 °C (red). (b) XRD patterns (from top to bottom) of an organogel formed by direct base addition to a PDD solution, bulk DBF, an organogel formed after base amplification (20 mM BPD, 0.6 M BA) at 40 °C, an organogel formed by direct addition of a BPD solution into a PDD solution containing DBF (0.62 M BPD, 0.6 M DBF), 1 hour after mixing 0.62 M BPD and 0.6 M DBF in solution, 8 hours after mixing 0.62 M BPD and 0.6 M DBF in solution. 1 mM TFA/DMSO was used as the solvent.

Since DSC measurements indicate some crystallinity in the base amplified systems, organogels formed after base amplification at 40 °C were further examined by X-ray diffraction (XRD). The dominant feature was an amorphous hump observed in Figure 8(a). Crystalline peaks were observed in the 2θ range from 4° to 14°, which increased with an increasing BA concentration, confirming presence of a BA-related crystalline phase. The organogels were then heated at 140 °C for 30 min and became liquid because of dissociation of catechol-Fe(III) complexes and melting of the crystalline phase. Samples also turned from dark purple to brown due to some catechol oxidation. Gels were recovered when the samples were cooled down and catechol-Fe(III) complexes reformed. The crystalline peak intensities did not fully recover, which corroborates the DSC results of reduced crystallinity after heating-cooling cycles. It is worth noting that the intensity difference of crystalline peaks in samples before and after heat treatment decreased with decreasing C_{BA} – in fact, the traces before and after heating almost overlapped when BA concentration was 0.2 M or less. As a control, a BA-free organogel was prepared by adding a BPD solution, which contains no crystalline phase as indicated by both DSC (Figure S5(a)) and XRD (Figure 8(b)).

DBF, a byproduct of base amplification, was synthesized and dissolved in a PDD + $FeCl_3$ solution (10 wt% PDD; catechol/Fe = 3/1, mol/mol), and a BPD solution was added to form an organogel. DSC analysis of the resultant gel revealed an endothermic melting peak at ~98 °C (Figure S5(b)). This melting peak shifted to a lower temperature in the second cycle with a decreased peak area, which agrees with what we observed for an organogel formed after base amplification. This sample also showed almost identical diffraction patterns to those of organogels formed after base amplification (Figure 8(b)). Given the susceptibility of DBF to self-polymerize, the following experiments were performed to rule out DBF polymerization as the primary mechanism for the observed organogel stiffening after base amplification. DSC was performed on bulk DBF over two cycles from 20 °C to 140 °C and back (Figure S5(c)). On the first heat, a sharp endothermic melting peak was observed at ~53 °C, followed by a broad exothermic peak likely indicative of self-polymerization of DBF. A tiny exothermic peak appeared during cooling around 45 °C, likely due to crystallization of residual unpolymerized DBF. No endothermic or exothermic features were observed in the second thermal cycle. In contrast, in the organogels formed after base amplification, a melting is observed at 112-116 °C, and a crystallization at 40-50 °C (Fig. S4). As we present in the following paragraph, it is probably a DBF-BPD adduct that is melting around 112-116 °C. The fact that crystallization is observed upon cooling, and melting on the following heat is strong indication DFB has not largely polymerized, even after heating to 140 °C. Therefore, we suggest that room temperature formation of poly(DBF) is very unlikely to be the reason for the high observed stiffness of the base amplified systems. To further confirm the identity of the crystalline phase, a mixture of BPD and DBF were characterized 1 hour and 8 hours after mixing. The diffraction patterns resembled that of the organogel formed after base amplification, and the intensities of the

crystalline peaks increased over time. In contrast, the BA- and DBF-free organogel formed by direct base addition did not show any crystallinity, and bulk DBF showed a different crystalline structure than the crystalline phase in the organogel formed after base amplification.

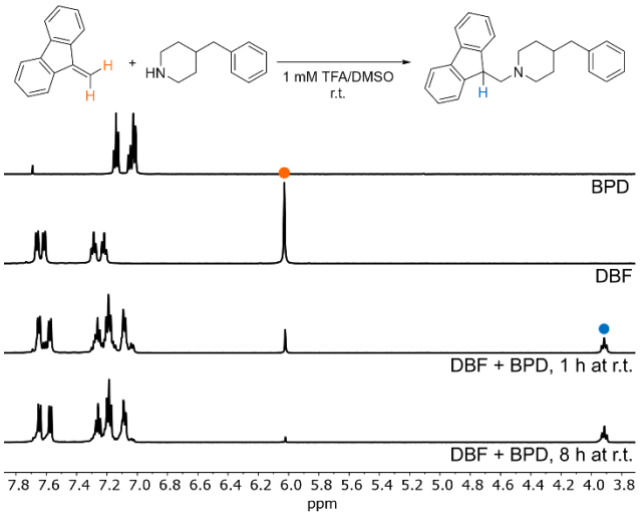

Figure 9. ^{1}H NMR spectra (from top to bottom) of BPD, DBF, a BPD-DBF mixture at t = 1 hour and t = 8 hours in $CDCl_3$. 0.62 M BPD and/or 0.6 M DBF were first dissolved in 1 mM TFA/DMSO and sampled for ^{1}H NMR.

DBF as a byproduct of Fmoc deprotection is known for the Michael-type addition reaction with an amine,[36] which was confirmed by ^{1}H NMR (Figure 9). After BPD and DBF were mixed, the DBF peak at ~6.02 ppm gradually decreased, and a new triplet appeared at ~3.91 ppm, indicating formation of an adduct from the two compounds. While little information about the DBF-BPD adduct can be found in literature, the melting point of the DBF-piperidine adduct, which has a similar structure, was reported to be 116-117 °C by Carpino *et al.*[37] and 107-109 °C by Akaji *et al.*,[38] in good agreement with our DSC results.

In summary, it was demonstrated that base amplification following a sub-threshold base trigger can successfully drive a macroscopic property change (e.g., gelation), as we showed using a solution of a catechol-bearing polymer and $FeCl_3$. The decoupling of stimuli amplification crosslinking reactions allows a myriad of combinations of reactions for sensitive responses, without the need of synthesizing specific and sometimes complex functionality. The utilization of a base amplifier also allows modulating gelation kinetics and final gel properties by different means. A higher concentration of either the base trigger (BPD) or base amplifier (BA) facilitated faster gelation of a catechol-bearing polymer solution containing Fe(III) with a shorter induction period. The plateau storage modulus of the formed organogel was proportional to BA concentration which decided final concentrations of the base and hence bis- and tris-catecholato-Fe(III) complexes. Additionally, the BA concentration determined the concentration of the DBF-BPD adduct that formed a crystalline phase contributing to the unusually high stiffness of the organogel. Hence, besides properties of the polymer backbone, an additional knob (i.e., physical properties of the reaction byproduct) can be utilized to tune material properties. We note, the samples described in this article were brittle because of the low polymer content deliberately used. Literature indicates that a higher polymer content might improve elasticity and flexibility of the resultant hybrid material.[39]

We note, the gradual loss of crystallinity and gel stiffness after heating-cooling cycles probably does result from self-polymerization of dibenzofulvene at an elevated temperature. It would be of interest to improve the reversibility of melting-crystallization and stiffness changes, structural modification of the Fmoc group to reduce the propensity of DBF derivatives for self-polymerization could be considered.

ASSOCIATED CONTENT

Supporting Information

The Supporting Information is available free of charge via the Internet at http://pubs.acs.org.
Synthesis and characterization methods; supplementary experimental results, figures, and tables.

AUTHOR INFORMATION

Corresponding Author

Paul V. Braun – *Department of Materials Science and Engineering, University of Illinois Urbana-Champaign, Urbana, IL 61801, United States; Department of Mechanical Science and Engineering, University of Illinois Urbana-Champaign, Urbana, IL 61801, United States; Materials Research Laboratory, University of Illinois Urbana-Champaign, Urbana, IL 61801, United States; Beckman Institute for Advanced Science and Technology, University of Illinois Urbana-Champaign, Urbana, IL 61801, United States;* Email: pbraun@illinois.edu

Authors

Shuqi Lai – *Department of Materials Science and Engineering, University of Illinois Urbana-Champaign, Urbana, IL 61801, United States; Materials Research Laboratory, University of Illinois Urbana-Champaign, Urbana, IL 61801, United States; Beckman Institute for Advanced Science and Technology, University of Illinois Urbana-Champaign, Urbana, IL 61801, United States*

Gaurav Chaudhary – *Department of Mechanical Science and Engineering, University of Illinois Urbana-Champaign, Urbana, IL 61801, United States; Materials Research Laboratory, University of Illinois Urbana-Champaign, Urbana, IL 61801, United States; Beckman Institute for Advanced Science and Technology, University of Illinois Urbana-Champaign, Urbana, IL 61801, United States*

Zhelong Jiang – *Department of Materials Science and Engineering, University of Illinois Urbana-Champaign, Urbana, IL 61801, United States; Materials Research Laboratory, University of Illinois Urbana-Champaign, Urbana, IL 61801, United States*

Randy H. Ewoldt – *Department of Mechanical Science and Engineering, University of Illinois Urbana-Champaign, Urbana, IL 61801, United States; Materials Research Laboratory, University of Illinois Urbana-Champaign, Urbana, IL 61801, United States; Beckman Institute for Advanced Science and Technology, University of Illinois Urbana-Champaign, Urbana, IL 61801, United States*

Present Addresses

Shuqi Lai – Intel Corporation
Gaurav Chaudhary – Intel Corporation
Zhelong Jiang – SLAC National Accelerator Laboratory, Stanford University

Notes

The authors declare no competing financial interest.

ACKNOWLEDGMENT

The authors would like to acknowledge support from the U.S. Department of Energy, Office of Basic Energy Sciences, Division of Materials Sciences and Engineering under Award # DE-SC0020858, through the Materials Research Laboratory at the University of Illinois Urbana-Champaign.

ABBREVIATIONS

BA, base amplifier; BPD, 4-benzylpiperidine; DBF, dibenzofulvene; DMSO, dimethylsulfoxide; Fmoc, 9-fluorenylmethyl; PDD, poly[di(ethylene glycol) methyl ether methacrylate-co-dopamine acrylamide]; TFA, trifluoroacetic acid; DSC, differential scanning calorimetry; NMR, nuclear magnetic resonance; UV-Vis, ultra-violet; XRD, X-ray diffraction.

REFERENCES

(1) Martin, P.; Hudspeth, A. J. Active Hair-Bundle Movements Can Amplify a Hair Cell ' s Response to Oscillatory Mechanical Stimuli. *Proc. Natl. Acad. Sci.* **1999**, *96* (25), 14306–14311.

(2) Mart'yanov, P. S.; Pustovoit, V. I.; Shorin, V. N. Electronic Amplifier for Modern Acousto-Optical Spectrometers. *J. Commun. Technol. Electron.* **2019**, *64* (8), 818–822. https://doi.org/10.1134/S1064226919080114.

(3) Choi, K.-B.; Lee, J. J.; Hata, S. A Piezo-Driven Compliant Stage with Double Mechanical Amplification Mechanisms Arranged in Parallel. *Sensors Actuators A Phys.* **2010**, *161* (1), 173–181. https://doi.org/https://doi.org/10.1016/j.sna.2010.05.027.

(4) Sun, X.; Reuther, J. F.; Phillips, S. T.; Anslyn, E. V. Coupling Activity-Based Detection, Target Amplification, Colorimetric and Fluorometric Signal Amplification, for Quantitative Chemosensing of Fluoride Generated from Nerve Agents. *Chemistry - A European Journal*. 2017, pp 3903–3909. https://doi.org/10.1002/chem.201604474.

(5) Goggins, S.; Frost, C. G. Approaches towards Molecular Amplification for Sensing. *Analyst* **2016**, *141* (11), 3157–3218. https://doi.org/10.1039/C6AN00348F.

(6) Baker, M. S.; Phillips, S. T. A Two-Component Small Molecule System for Activity-Based Detection and Signal Amplification: Application to the Visual Detection of Threshold Levels of Pd(II). *J. Am. Chem. Soc.* **2011**, *133* (14), 5170–5173. https://doi.org/10.1021/ja108347d.

(7) Kim, H.; Baker, M. S.; Phillips, S. T. Polymeric Materials That Convert Local Fleeting Signals into Global Macroscopic Responses. *Chem. Sci.* **2015**, *6* (6), 3388–3392. https://doi.org/10.1039/c5sc00701a.

(8) Mohapatra, H.; Kim, H.; Phillips, S. T. Stimuli-Responsive Polymer Film That Autonomously Translates a Molecular Detection Event into a Macroscopic Change in Its Optical Properties via a Continuous, Thiol-Mediated Self-Propagating Reaction. *J. Am. Chem. Soc.* **2015**, *137* (39), 12498–12501. https://doi.org/10.1021/jacs.5b08582.

(9) Bissette, A. J.; Fletcher, S. P. Mechanisms of Autocatalysis. *Angew. Chemie - Int. Ed.* **2013**, *52* (49), 12800–12826. https://doi.org/10.1002/anie.201303822.

(10) Mohapatra, H.; Schmid, K. M.; Phillips, S. T. Design of Small Molecule Reagents That Enable Signal Amplification via an Autocatalytic, Base-Mediated Cascade Elimination Reaction. *Chem. Commun.* **2012**, *48* (24), 3018–3020. https://doi.org/10.1039/c2cc17566e.

(11) Sella, E.; Shabat, D. Hydroquinone–Quinone Oxidation by Molecular Oxygen: A Simple Tool for Signal Amplification through Auto-Generation of Hydrogen Peroxide. *Org. Biomol. Chem.* **2013**, *11*, 5074–5078. https://doi.org/10.1039/c3ob40962g.

(12) Sun, X.; Shabat, D.; Phillips, S. T.; Anslyn, E. V. Self-Propagating Amplification Reactions for Molecular Detection and Signal Amplification: Advantages, Pitfalls, and Challenges. *J. Phys. Org. Chem.* **2018**, *31* (8), 1–9. https://doi.org/10.1002/poc.3827.

(13) Miyamoto, M.; Arimitsu, K.; Ichimura, K. Synthesis of Phenylsulfonylethyl Amplifier and Their Applications Carbamates as a Base to Photopolymer Systems. *J. Photopolym. Sci. Technol.* **1999**, *2*, 351–316.

(14) Arimitsu, K.; Miyamoto, M.; Ichimura, K. Synthesis of 9-Fluorenylmethyl and Their Applications Carbamates as a Base Amplifier to Photopolymer Systems Koji Arimitsu , Mana Mtyamoto and Kuaihiro Ichimura * of Resources of Technology , 4259 Nngatsuta , Japan Keywords : Autocatalytic Decomposition ,. *J. Photopolym. Sci. Technoloyg* **1999**, *12*, 317–318.

(15) Morikawa, Y.; Arimitsu, K.; Gunji, T.; Abe, Y.; Kunihiro Ichimura. Characteristics of Silicone Resins as Base Amplifiers and Their Applications to Photopatterning. *J. Photopolym. Sci. Technol.* **2003**, *16* (1), 81–82.

(16) Aoki, K.; Ichimura, K. Self-Developable Surface Relief Photoimaging Generated by Anionic UV-Curing of Epoxy Resins. *Polym. J.* **2009**, *41* (11), 988–992. https://doi.org/10.1295/polymj.PJ2009005R.

(17) Xu, Y.; Sen, S.; Wu, Q.; Zhong, X.; Ewoldt, R. H.; Zimmerman, S. C. Base-Triggered Self-Amplifying Degradable Polyurethanes with the Ability to Translate Local Stimulation to Continuous Long-Range Degradation. *Chem. Sci.* **2020**, *11* (12), 3326–3331. https://doi.org/10.1039/C9SC06582B.

(18) Aoki, K.; Hashimoto, T.; Ichimura, K. Synthesis of Novel Monodispersed Dendritic Base Amplifiers to Apply to Negative-Tone Photoresists. *J. Photopolym. Sci. Technol.* **2014**, *27* (4), 529–530.

(19) Arimitsu, K.; Ichimura, K. Nonlinear Organic Reaction of 9-Fluorenylmethyl Carbamates as Base Amplifiers to Proliferate Aliphatic Amines and Their Application to a Novel Photopolymer System. *J. Mater. Chem.* **2004**, *14*, 336. https://doi.org/10.1039/b311358b.

(20) Furutani, M.; Kakinuma, A.; Arimitsu, K. A Dismantlable Photoadhesion System Fabricated by an Anionic UV Curing of Epoxy Resins with a Base Amplifier Having a Disulfide Bond. *Polym. Chem.* **2018**, *56*, 237–241. https://doi.org/10.1002/pola.28898.

(21) Sinha, J.; Podgórski, M.; Tomaschke, A.; Ferguson, V. L.; Bowman, C. N. Phototriggered Base Amplification for Thiol-Michael Addition Reactions in Cross-Linked Photopolymerizations with Efficient Dark Cure. *Macromolecules* **2020**, *53* (15), 6331–6340. https://doi.org/10.1021/acs.macromol.0c00776.

(22) He, M.; Huang, X.; Zeng, Z.; Yang, J. Phototriggered Base Proliferation: A Highly Efficient Domino Reaction for Creating Functionally Photo-Screened Materials. *Macromolecules* **2013**, *46* (16), 6402–6407. https://doi.org/10.1021/ma400983t.

(23) He, M.; Jiang, S.; Xu, R.; Yang, J.; Zeng, Z.; Chen, G. Domino Free Radical Photopolymerization Based on Phototriggered Base Proliferation Reaction and Redox Initiation. *J. Polym. Sci. Part A Polym. Chem.* **2014**, *52* (11), 1560–1569. https://doi.org/10.1002/pola.27149.

(24) Xu, Y.; Morado, E. G.; Zimmerman, S. C. Construction from Destruction Using a Photo-Triggered Self-Propagating Degradable Polyurethane as a One-Pot Epoxy. *Polym. Chem.* **2020**, *11* (38), 6215–6220. https://doi.org/10.1039/D0PY00779J.

(25) Holten-Andersen, N.; Harrington, M. J.; Birkedal, H.; Lee, B. P.; Messersmith, P. B.; Lee, K. Y. C.; Waite, J. H. PH-Induced Metal-Ligand Cross-Links Inspired by Mussel Yield Self-Healing Polymer Networks with near-Covalent Elastic Moduli. *Proc. Natl. Acad. Sci.* **2011**, *108* (7), 2651–2655.

https://doi.org/10.1073/pnas.1015862108.
(26) Jin, H.; Mangun, C. L.; Griffin, A. S.; Moore, J. S.; Sottos, N. R.; White, S. R. Thermally Stable Autonomic Healing in Epoxy Using a Dual-Microcapsule System. *Adv. Mater.* **2014**, *26* (2), 282–287. https://doi.org/10.1002/adma.201303179.
(27) Possanza Casey, C. M.; Moore, J. S. Base-Triggered Degradation of Poly(Vinyl Ester Sulfone)s with Tunable Sensitivity. *ACS Macro Lett.* **2016**, *5* (11), 1257–1260. https://doi.org/10.1021/acsmacrolett.6b00698.
(28) Sasaki, T.; Kondo, T.; Noro, M.; Saida, K.; Yaguchi, H.; Naka, Y. Photoinduced Depolymerization in Poly(Olefin Sulfone) Films Comprised of Volatile Monomers Doped with a Photobase Generator. *J. Polym. Sci. Part A Polym. Chem.* **2012**, *50* (8), 1462–1468. https://doi.org/10.1002/pola.25898.
(29) Bijlsma, J.; de Bruijn, W. J. C.; Hageman, J. A.; Goos, P.; Velikov, K. P.; Vincken, J.-P. Revealing the Main Factors and Two-Way Interactions Contributing to Food Discolouration Caused by Iron-Catechol Complexation. *Sci. Rep.* **2020**, *10* (1), 8288. https://doi.org/10.1038/s41598-020-65171-1.
(30) Xu, H.; Nishida, J.; Ma, W.; Wu, H.; Kobayashi, M.; Otsuka, H.; Takahara, A. Competition between Oxidation and Coordination in Cross-Linking of Polystyrene Copolymer Containing Catechol Groups. *ACS Macro Lett.* **2012**, *1* (4), 457–460. https://doi.org/10.1021/mz200217d.
(31) Guo, Z.; Ni, K.; Wei, D.; Ren, Y. Fe3+-Induced Oxidation and Coordination Cross-Linking in Catechol–Chitosan Hydrogels under Acidic PH Conditions. *RSC Adv.* **2015**, No. 2, 37377–37384. https://doi.org/10.1039/C5RA03851K.
(32) Miller, K. A.; Morado, E. G.; Samanta, S. R.; Walker, B. A.; Nelson, A. Z.; Sen, S.; Tran, D. T.; Whitaker, D. J.; Ewoldt, R. H.; Braun, P. V.; Zimmerman, S. C. Acid-Triggered, Acid-Generating, and Self-Amplifying Degradable Polymers. *J. Am. Chem. Soc.* **2019**, *141* (7), 2838–2842. https://doi.org/10.1021/jacs.8b07705.
(33) Kumar, R.; Liu, Z.; Lokitz, B.; Chen, J.; Carrillo, J.-M.; Jakowski, J.; Collier, C. P.; Retterer, S.; Advincula, R. Harnessing Autocatalytic Reactions in Polymerization and Depolymerization. *MRS Commun.* **2021**, *11* (4), 377–390. https://doi.org/10.1557/s43579-021-00061-9.
(34) Mora, E.; Artavia, L. D.; Macosko, C. W. Modulus Development during Reactive Urethane Foaming. *J. Rheol. (N. Y. N. Y).* **1991**, *35*, 921. https://doi.org/10.1122/1.550163.
(35) Neff, R. A.; Macosko, C. W. Simultaneous Measurement of Viscoelastic Changes and Cell Opening during Processing of Flexible Polyurethane Foam. *Rheol. Acta* **1996**, *35* (6), 656–666. https://doi.org/10.1007/BF00396514.
(36) Sheppeck II, J. E.; Kar, H.; Hong, H. A Convenient and Scaleable Procedure for Removing the Fmoc Group in Solution. **2000**, *41*, 5329–5333.
(37) Carpino, L. A.; Han, G. Y. The 9-Fluorenylmethoxycarbonyl Amino-Protecting Group. *J. Org. Chem.* **1972**, *37* (22), 3404. https://doi.org/10.1021/jo01335a600.
(38) Akaji, K.; Teruya, K.; Akaji, M.; Aimoto, S. Synthesis of Cyclic RGD Derivatives via Solid Phase Macrocyclization Using the Heck Reaction. *Tetrahedron* **2001**, *57* (12), 2293–2303. https://doi.org/10.1016/S0040-4020(01)00113-2.
(39) Yang, F. (Kuo); Cholewinski, A.; Yu, L.; Rivers, G.; Zhao, B. A Hybrid Material That Reversibly Switches between Two Stable Solid States. *Nat. mat* **2019**, *18* (August), 874–882. https://doi.org/10.1038/s41563-019-0434-0.

TOC graphic

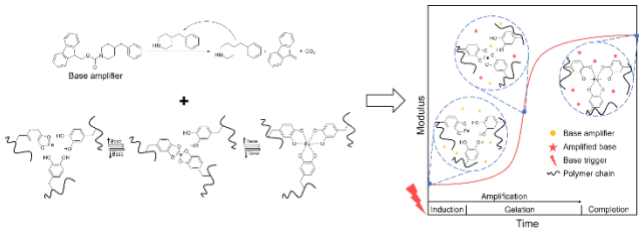
Base amplifier
Modulus
Base amplifier
Amplified base
Base trigger
Polymer chain
Amplification
Induction
Gelation
Completion
Time